Published in final edited form as:
Cell Cycle. 2009 May 15; 8(10): 1589–1602.

AKT1 mediates bypass of the G_1/S checkpoint after genotoxic stress in normal human cells

Madhu A. Lal[1,3,†], **Dongsoon Bae**[1,†], **Tura C. Camilli**[1,3,‡], **Steven R. Patierno**[1,2,3,4], and **Susan Ceryak**[1,2,3,4,*]

[1]Department of Pharmacology and Physiology, The George Washington University Medical Center; Washington DC, USA

[2]Department of Medicine, The George Washington University Medical Center; Washington DC, USA

[3]Program in Molecular Oncology, The George Washington University Medical Center; Washington DC, USA

[4]GW Cancer Institute, The George Washington University Medical Center; Washington DC, USA

Abstract

Certain forms of hexavalent chromium [Cr(VI)] are human carcinogens. Our recent work has shown that a broad range protein tyrosine phosphatase (PTP) inhibitor, sodium orthovanadate (SOV), abrogated both Cr(VI)-induced growth arrest and clonogenic lethality. Notably, SOV enhanced Cr(VI) mutation frequency, ostensibly through forced survival of genetically damaged cells. In the present study, co-treatment with this PTP inhibitor bypassed the Cr(VI)-induced G_1/S checkpoint arrest in diploid human lung fibroblasts (HLF). Moreover, the PTP inhibitor abrogated the Cr(VI)-induced decrease in the expression of key effectors of the G_1/S checkpoint [Cyclin D1, phospho Ser 807/811 Rb (pRB), p27]. Cr(VI)-induced G_1 arrest was associated with the cytoplasmic appearance of pRb and the nuclear localization of p27, both of which were reversed by the PTP inhibitor. The PTP inhibitor's reversal of G_1/S checkpoint effector localization after Cr exposure was found to be Akt1-dependent, as this was abrogated by transfection with either akt1 siRNA or an Akt1-kinase dead plasmid. Furthermore, Akt1 activation alone was sufficient to induce G_1/S checkpoint bypass and to prevent Cr(VI)-induced changes in pRb and p27 localization. In conclusion, this work establishes Akt1 activation to be both sufficient to bypass the Cr(VI)-induced G_1/S checkpoint, as well as necessary for the observed PTP inhibitor effects on key mediators of the G_1/S transition. The potential for Akt to bypass G_1/S checkpoint arrest in the face of genotoxic damage could increase genomic instability, which is a hallmark of neoplastic progression.

Keywords

Akt1; hexavalent chromium; G_1/S checkpoint transition; cdk inhibitors

*Correspondence to: Susan Ceryak; Department of Pharmacology and Physiology; The George Washington University; 2300 I Street; N.W., Room 650; Ross Hall; Washington DC 20037 USA; Tel.: 202.994.3896; Fax: 202.994.2870; phmsmc@gwumc.edu.
†These authors contributed equally to this work.
‡Current address: Laboratory of Immunology; National Institute on Aging; National Institutes of Health; Baltimore, MD USA

Note
Supplementary materials can be found at: www.landesbioscience.com/supplement/LalCC8-10-Sup.pdf

Introduction

Uncontrolled cell proliferation after genotoxic injury can contribute to the development of a transformed phenotype. The establishment of cell cycle checkpoints in response to genotoxic stress is essential for the maintenance of genomic integrity. As a barrier to uncontrolled proliferation, the G_1/S transition is halted in response to growth-inhibiting stimuli, DNA damage and inappropriate activation of oncogenes.[1] Consequently, bypass of the G_1/S checkpoint in the face of DNA damage may facilitate the acquisition of certain genetic/epigenetic characteristics that could provide cells with a selective growth advantage and predispose them to neoplastic progression.[2]

There is considerable evidence that protein tyrosine phosphorylation is responsible for the maintenance of proliferative signals and is involved in the early stages of neoplasia.[3] While protein tyrosine phosphorylation is implicated in the maintenance of proliferative signals, protein tyrosine phosphatases (PTPs) have an opposing role.[3] PTPs such as PTEN (phosphatase and tensin homolog deleted on chromosome ten) and MKP (MAP kinase phosphatase) are integral components of the Akt and Erk survival pathways, and are responsible for their respective inactivation.[4,5] Indeed, certain of these PTPs have been described as tumor suppressors since their overall effect is to decrease cell proliferation.[6,7]

Vanadium compounds such as sodium orthovanadate have been found to inhibit PTEN via its tyrosine phosphorylation resulting in Akt activation.[8,9] Sodium orthovanadate (SOV) is known to cause an increase in protein tyrosine phosphorylation, leading to augmentation of cell proliferation.[10] We have found that maintenance of protein tyrosine phosphorylation through PTP inhibition by SOV increases clonogenic survival in the presence of Cr(VI)-induced genotoxic insult, mainly due to the lack of a protracted growth arrest after Cr(VI) treatment. Importantly, this PTP inhibitor enhanced Cr(VI)-induced mutation frequency at the hypoxanthine-guanine phosphoribosyltransferase (HPRT) locus.[11]

The progression of cells through the G_1/S checkpoint and into S-phase is controlled by a number of positive and negative factors.[12] The CyclinD-cdk4/6 complexes regulate early G_1 progression, whereas the Cyclin E/cdk2 complex is responsible for the hyperphosphorylation and consequent inactivation of Rb, which promotes the transcription of S-phase genes by release of the E2-F transcription factor.[13] Rb inactivation by phosphorylation is considered to be the “point of no return”, after which passage through the cell cycle through mitosis can not be reversed.[14] The cyclin-cdk complexes are subject to another level of control by the expression and localization of cdk inhibitors, p21 and p27.[15] In many cancer cells, frequent alterations in G_1/S checkpoint effectors (i.e., Cyclin D1, p21 and p27) are observed resulting in an inability of cells to arrest at the G_1/S checkpoint after DNA damage.[16]

Certain forms of hexavalent chromium [(Cr(VI)] are known human respiratory carcinogens that can be employed as useful genotoxic tools with clear environmental and toxicological importance. We utilized this respiratory carcinogen as a model genotoxin to investigate mechanisms of checkpoint bypass which in turn could lead to carcinogenesis. The structural and functional aspects of Cr(VI)-induced DNA damage are summarized in several review articles.[17–20] Environmental and occupational exposure to chromate continues to loom large as a major public health issue and a source of continuous high-profile litigation.

The overall objective of this present study was to elucidate the role of Akt in the bypass of the G_1/S checkpoint after genotoxic stress. We tested the hypothesis that the Cr(VI)-induced G_1/S checkpoint arrest can be bypassed by Akt activation, and this bypass results in the modulation of expression and localization of G_1/S transition effectors. Our data suggest that activation of Akt, by either PTP inhibition or transfection with constitutively active

myristoylated (Myr)Akt1, results in a bypass of the G_1/S checkpoint after Cr(VI) exposure. This checkpoint bypass was accompanied by changes in the localization and expression of the G_1/S effectors, p27 and phospho Ser 807/811 Rb (pRb). Moreover, in the presence of Akt downregulation, PTP inhibition was unable to rescue the cells from the Cr(VI)-induced effects on the localization of pRb and p27, indicating the need for Akt activity in the PTP inhibitor effect. Taken together, our data highlight a role for Akt1 in the loss of G_1/S checkpoint control after genotoxic exposure by phosphotyrosine-regulated survival signaling which, in turn, may lead to genomic instability and carcinogenesis.

Results

G_1/S checkpoint arrest is bypassed by PTP inhibition with SOV

Our previous data indicated that PTP inhibition by SOV maintained tyrosine phosphorylation, increased clonogenic survival via override of growth arrest after Cr(VI) exposure, and enhanced Cr(VI)-induced mutagenesis in HLF cells.[11] To elucidate the impact of PTP inhibition on the G_1/S checkpoint, we analyzed the G_1/S transition in HLF cells 24 h after exposure to Cr(VI) in the presence and absence of SOV. G_1/S checkpoint function was assessed by measuring the entry of cells into S-phase by BrdU and PI double staining. We confirmed BrdU DNA incorporation by immunofluorescence staining as shown in Figure 1A. PI staining was used to indicate the position of the nucleus. In the control (non Cr-treated) cells, BrdU staining was localized to the nucleus, consistent with its incorporation into replicating DNA, with 50% of the cells staining positive for BrdU nuclear incorporation. Following 24 h Cr(VI) exposure, BrdU nuclear incorporation was no longer observed in any of the cells. In sharp contrast, BrdU staining was maintained after co-treatment with the PTP inhibitor and Cr(VI), with approximately 35% of cells in the field positive for BrdU incorporation. Finally, PTP inhibition with SOV treatment alone had no effect on nuclear BrdU staining, with approximately 42% of cells in the field positively staining for BrdU incorporation, as observed in the control cells.

We have previously found that 24 h Cr(VI) exposure was associated with a G_1/S checkpoint arrest in HLFs, as assessed by BrdU incorporation into early S phase cells.[22] In order to further explore the effect of PTP inhibition on G_1/S transition, we studied BrdU incorporation, as a function of PI staining by flow cytometry. As shown in Figure 1B, the percentage of cells in early S-phase (R5 gate), as indicated by the incorporation of BrdU, was 5.6% in the control. The addition of SOV alone had no effect on S-phase progression, with 5.4% of the total cells in early S phase. Exposure of the cells to 1 μM Cr(VI) resulted in a G_1/S checkpoint arrest, as the cells in early S-phase decreased to ~30% of the non-treated control. However, PTP inhibition by SOV markedly abrogated the Cr-induced G_1/S checkpoint arrest, as shown by the nearly two-fold increase in the percentage of cells in early S phase (55% of the respective control, Fig. 1C).

The PTP inhibitor-induced bypass of the G_1/S checkpoint is associated with changes in pRb and cyclin D1 protein expression and pRb cellular localization

Because SOV co-treatment bypassed the G_1/S checkpoint after Cr(VI) exposure, we studied the protein expression of the key G_1/S checkpoint effectors, Rb and cyclin D1 after Cr(VI) exposure in the presence and absence of the PTP inhibitor. As shown in Figure 2A, after 24 h exposure, Cr(VI) induced a concentration-dependent decrease in both phospho Ser807/811 Rb (pRb) and cyclin D1 expression, consistent with a G_1/S checkpoint arrest. The PTP inhibitor alone had no effect on either pRb or cyclin D1 protein expression. However, SOV co-treatment abrogated the Cr-induced decrease in protein expression of these G_1/S effectors. Total Rb showed a similar pattern of expression with both agents.

G_1/S checkpoint transition is also controlled by cellular localization of its effector proteins.[23] Therefore, we determined the effect of Cr(VI) and PTP inhibition on the localization of pRb and cyclin D1 by immunofluorescence staining. PI was used as a marker to indicate nuclear staining. As shown in Figure 2B, in control cells, pRb was exclusively localized to the nucleus as evidenced by bright, uniform nuclear staining in 100% of the cells studied. Exposure of HLFs to 1 and 3 μM Cr(VI) induced the cytosolic localization of pRb with a significant decrease in exclusive nuclear pRb staining, which was observed in only 25 and 20% of the cells, respectively ($p < 0.001$). Interestingly, nuclear pRb staining was more punctuate in the presence of Cr(VI) (Fig. 2B and Suppl. Fig. 1). In the absence of Cr(VI) treatment, the PTP inhibitor alone had no effect on pRb localization. However, the Cr(VI)-induced cytoplasmic localization of pRb was abrogated by the PTP inhibitor, as 100% of the cells treated with 1 and 3 μM Cr(VI) and 10 μM SOV exhibited exclusive uniform and bright nuclear staining, similar to the controls. Neither Cr(VI) nor SOV had any effect on the localization of Cyclin D1, which was found to be in the nucleus under all conditions, indicating that alterations in protein localization were protein-specific and not the result of a general effect of the PTP inhibitor (data not shown).

The PTP inhibitor-induced bypass of the G_1/S checkpoint is associated with changes in p27 protein expression and cellular localization

Since cdk inhibitors are important mediators of G_1/S arrest, we determined the effect of PTP inhibition on Cr(VI)-induced changes in protein expression of the cdk inhibitor, p27. Interestingly, Cr(VI) induced a concentration-dependent decrease in p27 protein expression after 24 h exposure as shown in Figure 3A. The PTP inhibitor alone had no effect on p27 protein expression but significantly reversed the Cr(VI)-induced decrease in p27 protein expression. Notably, neither Cr(VI) nor SOV had any effect on p21 protein expression (data not shown).

Nuclear localization of p27 is necessary to block Rb phosphorylation by the Cyclin E/cdk2 complex, which in turn leads to a G_1/S arrest.[24] Therefore, we determined the effect of Cr(VI) and PTP inhibition on the cellular localization of p27. As shown in Figure 3B 100% of control cells exhibited a uniform distribution of p27 throughout the nucleus and the cytosol. After 24 h treatment with 1 and 3 μM Cr(VI) there was an increased accumulation of p27 in the nucleus versus the cytosol, with only 2 and 1% of the respective treated cells displaying cytoplasmic p27, as compared to the control ($p < 0.001$). SOV alone had no effect on the cellular distribution of p27 compared to that of the control, with 100% of the cells showing nucleo-cytoplasmic p27 distribution. However, the PTP inhibitor abrogated the Cr-induced nuclear accumulation of p27, and 96 and 95% of the cells co-treated with SOV and 1 and 3 μM Cr(VI), respectively, stained uniformly for p27 throughout the cell. These findings were confirmed by immunoblotting studies of subcellular fractions as shown in Figure 3C. In keeping with the immunofluorescence data, the PTP inhibitor decreased the ratio of nuclear/cytosolic p27 protein by ~50% of that observed in the presence of 3 μM Cr(VI) alone. Finally, neither Cr(VI) nor SOV had any effect on the localization of p21, which was found to be localized to the nucleus under all conditions (data not shown).

PTP inhibition abrogates the Cr(VI)-induced decrease in Akt expression and activity

Since the PTP inhibitor induced a 2-fold increase in G_1/S transition after treatment with Cr(VI), we postulated that the mechanism of checkpoint bypass by PTP inhibition was through upregulation of survival signaling pathways. Previous studies by our laboratory and others [5] have found SOV to enhance tyrosine phosphorylation in vitro and vivo. In addition, SOV-induced PTP inhibition has been shown to activate the Akt pathway via tyrosine phosphorylation and downregulation of the inhibitor, PTEN [8,9,2] In the present study, we also observed that tyrosine phosphorylation of PTEN was increased by over 3-fold as early

as 1 h in the presence of SOV. Furthermore, we also immunoprecipitated PTEN and looked at tyrosine phosphorylation in the PTEN immunoprecipitates. We observed a 2-fold increase in tyrosine phosphorylation in the presence of SOV as early as 1 hour post treatment (Fig. 4A).

The increased PTEN tyrosine phosphorylation observed after PTP inhibition suggested that (1) PTEN may be inhibited by SOV, and (2) that the Akt pathway may be involved in the SOV-induced bypass of the G_1/S checkpoint. Therefore, we determined the effect of the PTP inhibitor on Akt pathway activation. As shown in Figure 4B, 24 h treatment of cells with 1–6 μM of Cr(VI) resulted in a significant, concentration-dependant, 25–75% decrease in the expression of pSer473 Akt. This decrease in activated Akt was significantly abrogated by PTP inhibition (i.e., 10 μM SOV).

We next examined Akt in vitro activation after Cr(VI) exposure in the presence and absence of the PTP inhibitor. Akt immunoprecipitates were used to phosphorylate GSK3α/β in vitro. Akt kinase activity towards GSK3, as expressed as the amount of GSK3 phosphorylated by Akt and normalized to total GSK3, was significantly decreased, in a concentration-dependant fashion after treatment with 1–6 uM Cr(VI) (Fig. 4C). Notably, the Cr(VI)-induced downregulation in Akt activity was significantly abrogated by the PTP inhibitor (Fig. 4C). These results show that Akt activity is preserved in the presence of genotoxic stress via maintenance of tyrosine phosphorylation by the PTP inhibitor, SOV.

Akt is necessary for the PTP inhibitor-induced abrogation of Cr(VI)-induced effects on the localization of pRb and p27

The ability of the PTP inhibitor to partially abrogate Cr-induced Akt downregulation, prompted us to study the role of Akt in the SOV-induced G_1/S checkpoint bypass after Cr exposure. HLF cells were transiently transfected with the Akt1 kinase-dead mutant plasmid construct (Akt1-KD). Transfection of the Akt1-KD construct was associated with a 47–59% decrease in pan-AKT Ser 473 phosphorylation (i.e., activation) 48 h post transfection (Suppl. Fig. 2).

We studied the impact of Akt downregulation on the PTP inhibitor-induced relocalization of the G_1/S transition effectors, pRb and p27 after Cr(VI) exposure (Fig. 5). As shown in Figure 5A (upper), in vector control-transfected cells, similar to the untransfected control cells (Fig. 3B, lower), treatment with 10 μM SOV abrogated the Cr(VI)-induced cytoplasmic localization of Rb in 100% of the cells treated with either 1 or 3 μM Cr(VI). In sharp contrast, in cells transfected with the Akt1-KD plasmid, the PTP inhibitor was no longer able to abrogate the Cr(VI)-induced effects on pRb localization and only 7 and 17% of the cells respectively co-treated with SOV and 1 and 3 μM Cr(VI) maintained exclusive pRb nuclear staining (Fig. 5A, lower).

We next studied the role of Akt in the abrogation of Cr(VI)-induced nuclear localization of p27 by PTP inhibition. As shown in Figure 5B, treatment of vector control-transfected cells with 1 and 3 μM Cr(VI) in the presence of the PTP inhibitor resulted in 100% of cells displaying a uniform, nucleo-cytoplasmic distribution of p27, similar to the observed effect of the PTP inhibitor on untransfected cells (Fig. 3B, lower). However, cells transfected with the Akt1-KD construct and co-treated with 1 and 3 μM Cr(VI) and 10 μM SOV under the same conditions resulted in the nuclear accumulation of p27, with only 0–2% of the cells displaying cytoplasmic p27. Similar results with p27 localization after Akt downregulation with Akt1 siRNA, are shown in Supplementary Figure 3.

AKT is sufficient for G_1/S checkpoint bypass and G_1/S effector re-localization after Cr(VI) exposure

Our genetic studies indicated that Akt1 inhibition/inactivation abrogated the ability of the PTP inhibitor to re-localize the G_1/S effectors, Rb and p27 after Cr(VI) exposure, thereby leading us to conclude that Akt1 was necessary for the PTP inhibitor-induced G_1/S bypass after DNA damage. To determine whether Akt was sufficient for G_1/S checkpoint bypass, we analyzed the G_1/S transition in HLFs after Cr(VI) exposure (24 h) in cells transfected with a constitutively active Akt1 gene, which contains a Src N-terminal myristoylation sequence (Myr-Akt1)[27] Myr-Akt1 transfection was associated with a 4.5-fold increase in pSer 473 pan Akt (Suppl. Fig. 2), as well as a 1.6-fold increase in Gsk3β phosphorylation (data not shown).

G_1/S checkpoint function after constitutive Akt1 activation was assessed by measuring the delay in entry of cells into S-phase by BrdU and PI double staining. We measured BrdU DNA incorporation by immunofluorescence staining as shown in Figure 6A. PI staining was used to indicate the position of the nucleus. In the vector-transfected, non Cr(VI)-treated cells, BrdU staining was localized to the nucleus and stained it in a bright uniform manner with 37% of cells staining positive for BrdU incorporation. Following 24 h Cr(VI) exposure, BrdU nuclear incorporation was weakly observed in 8% of the vector transfected cells. In sharp contrast, BrdU staining was maintained in Myr-Akt1 transfected cells treated with Cr(VI) with 30% of the cells staining for BrdU. Finally, 47% of the cells transfected with Myr-Akt1 stained positive for BrdU incorporation. We further assessed G_1/S checkpoint activation as a function of BrdU incorporation by flow cytometry with PI double staining. Figure 6B shows that the number of cells in early S-phase in vector-transfected cells treated with 1 μM Cr(VI) was 60% of that observed in the untreated vector-transfected cells. However, in the cells transfected with Myr-Akt1 and treated with 1 μM Cr(VI), the proportion of cells in early S-phase was approximately 120% of its respective control.

We then studied the effect of constitutive Akt activation on pRb localization after Cr(VI) exposure. As shown in Figure 6C, in cells transfected with the mock vector, 100% of the cells exhibited exclusive nuclear pRb localization, similar to the untransfected cells (Fig. 2B). Moreover, treatment with Cr(VI) caused cytoplasmic redistribution of pRb with just 2–5% of the cells displaying nuclear staining. In sharp contrast, in cells transfected with Myr-Akt1, Cr(VI) treatment did not cause cytoplasmic localization of pRb. Instead, pRb remained predominantly nuclear in 100 and 98% of cells treated with 1 and 3 μM Cr(VI), respectively.

We also investigated the effect of Akt activation on the nuclear localization of p27 (Fig. 6C). In the mock vector-transfected cells, 100% of the cells observed exhibited nucleocytoplasmic staining of p27, similar to that seen in the untransfected control cells (Fig. 2C). Likewise, after treatment with 1 and 3 μM Cr(VI), p27 localization was exclusively nuclear, as none of the cells (0%) exhibited p27 cytoplasmic staining. However, in cells transfected with Myr-Akt1, following 1 and 3 uM Cr(VI) treatment, p27 was evenly distributed throughout the cell with a respective 97 and 95% of the cells treated with 1 and 3 μM Cr(VI) showing nucleo-cytoplasmic distribution of p27. These data were confirmed by immunoblotting of nuclear and cytosolic cell fractions in cells transfected with Myr-Akt1 as compared to the mock vector control-transfected cells (Fig. 6D). The ratio of nuclear/cytoplasmic p27 was approximately 12.5% of the ratio observed in vector transfected cells.

Discussion

Protein tyrosine phosphatases (PTPs) are integral components of key survival pathways, and are responsible for their inactivation. Our recent studies found that PTP inhibition with SOV

enhanced clonogenic survival and mutation frequency after Cr(VI) exposure in normal diploid mammalian cells, through a mechanism involving an override of Cr(VI)-induced growth arrest.[11] The studies presented here describe a mechanism for PTP inhibitor-induced G_1/S checkpoint bypass by Akt1 after Cr(VI) exposure. Moreover, our data indicated that Akt activation alone is sufficient to induce S phase entry in the face of genotoxic stress. The Akt-mediated checkpoint bypass was accompanied by changes in the localization and expression of G_1/S effectors, pRb, cyclin D1 and p27. Taken together, our data suggest a critical role for Akt1 at the G_1/S checkpoint in cell cycle progression which can occur downstream of tyrosine phosphorylation-regulated pathways. These results underscore the potential for genomic instability as a result of loss of checkpoint control and highlight a potential role for PTPs in early neoplastic progression after initial genotoxic stress.

There is considerable evidence that dysregulated protein tyrosine phosphorylation is responsible for the maintenance of proliferative signals and is involved in the early stages of neoplasia.[3,28–30] Consequently, certain PTPs have been described as tumor suppressors since their overall effect is to decrease cell proliferation and they have been regarded to have target potential.[6,7] Notably, our study is the first to report that PTP inhibition results in a non-lethal bypass of G_1/S checkpoint arrest in the face of genotoxic insult. This bypass of the Cr(VI)-induced G_1/S checkpoint was not related to a difference in Cr-DNA binding, as PTP inhibition has no effect on either Cr uptake or Cr-DNA adduct levels.[11] Previous reports have found SOV-induced PTP inhibition to enhance S phase progression in murine 3T3 and epithelial cells,[31,32] although SOV treatment alone had no apparent effect on cell proliferation at concentrations ≤10 μM in the present studies.

SOV has been shown to activate tyrosine phosphorylation in vivo, in association with its PTP inhibitory activity[25,33] which we have also found in a recent study.[11] SOV has been reported to activate both AKT and ERK pathways[8,34–38] which is presumably through PTP inhibition, highlighting a role for tyrosine phosphorylation in the regulation of cell survival. PTEN is a lipid and tyrosine phosphatase that is responsible for the inactivation of PI3 kinase, and its downstream target, Akt.[39,40] SOV as well as other vanadium compounds have been shown to maintain PTEN tyrosine phosphorylation, and consequently inhibit its activity, resulting in Akt activation.[8,40] In keeping with these reports, we also found that as early as 1 h after treatment with SOV, there was a ~4-fold increase in tyrosine phosphorylation of PTEN. This is consistent with our findings in the present study, that the Cr(VI)-induced concentration-dependent decrease in both phospho-Ser-473 Akt expression and Akt in vitro activity was significantly abrogated by the PTP inhibitor. Interestingly, the ability of Cr(VI) to downregulate Akt activity has been previously reported, albeit with much higher concentrations (50 μM) of Cr(VI).[41] The mechanism of Cr(VI)-induced Akt downregulation is currently under investigation in our laboratory. Importantly, we did not observe any effect of SOV on ERK activation in the present study (data not shown). Therefore, it remains possible that upstream phosphotyrosine kinases may promote G_1/S transit after PTP inhibition and genotoxin exposure through pathways exclusively upstream of AKT, and potentially involving PTEN. This is further supported by our observation that constitutive activation of Akt was sufficient to bypass the G_1/S checkpoint.

The retinoblastoma (Rb) protein, being a negative regulator of cell growth, is frequently inactivated/mutated in human cancers.[42] Hyperphosphorylation of Rb is concomitant with the G_1/S transition and entry into the S-phase whereas hypophosphorylated pRb is considered to be the active form and is predominantly seen in cells that are arrested in G_1.[43] Rb phosphorylation is considered to be the “point of no return” in G_1/S cell cycle transition and is directly phosphorylated by the complex of Cyclin D1 and cdk4/6.[24] Sequential phosphorylation of at least sixteen Cdk phosphorylatable serine/threonine residues leads to inactivation of the Rb protein. Specifically, phosphorylation on the Ser 807/811 residue is

important in the transition from G_1 to S.[42] Data from the present study indicate that Cr(VI) induced a decrease in Rb Ser807/811 phosphorylation, consistent with a G_1/S checkpoint arrest. Importantly, this Cr-induced decrease in pRb expression was not seen in the presence of the PTP inhibitor. Cyclin D1 protein expression is also required to drive cell cycle progression.[14] It has been reported that in the face of cell cycle arrest, Cyclin D1 levels are decreased, while increased cell proliferation corresponds to an increased level of Cyclin D1 expression.[44] In keeping with those data, our results show that Cr(VI) induced a decrease in Cyclin D1 levels which was significantly reversed by PTP inhibition.

Cytoplasmic localization of phosphorylated Rb is seen in many human cancers.[42] There are previously published reports of nucleo-cytoplasmic shuttling of pRb in cells in which cdk4 has been mutated.[42] In the present work, in normal human lung fibroblasts, we found that Cr(VI) exposure was associated with a punctate nuclear staining of pRb accompanied by cytoplasmic localization that was reversed by Akt activation. It has been previously reported that vanadate-induced Akt activity was blocked in cells that were transfected with a dominant negative Akt kinase mutant plasmid.[45] Our data is consistent with these reports. In the present study, in cells transfected with the Akt1 kinase dead mutant plasmid, the PTP inhibitor effect on pRb localization in cells treated with Cr(VI) was abrogated. This highlights the requisite role of Akt in mediating the PTP inhibitor effects on pRb localization, during genotoxic stress.

Other effectors of the G_1/S checkpoint are the cdk inhibitors, p21 and p27. Increased levels of expression of p21 and p27 have been shown to be concomitant with a cell cycle arrest in G_1.[46] In addition, the expression of both p21 and p27 can be stimulated in response to anti-proliferative signals, and thus block the G_1/S transition.[47] Loss of either p21 or p27 has been shown to confer cells with a proliferative advantage.[48] In contrast to the above mentioned reports, our data show that in response to treatment with Cr(VI), the expression of p27 was decreased and this was significantly reversed by PTP inhibition. Moreover, neither Cr(VI) nor SOV had any effect on the levels of p21 protein expression. However, previous work in our laboratory has shown that after treatment with Cr(VI), p21 mRNA levels are significantly increased while p27 mRNA levels remain unchanged.[49] This apparent discrepancy might be the result of Cr(VI) likely targeting p27 for degradation. Previous reports have found that both p27 and p21 have cdk2-independent activities.[50] This could explain our finding that although Cr(VI) causes a decrease in p27 protein expression levels, we observed a G_1/S cell cycle arrest owing to its exclusive nuclear localization. Consistent with our findings in the present study, the function of p27 as a cdk inhibitor has been reported to be governed more by its localization, than by its expression.[51]

Spatial and temporal control of protein expression and activity governs protein function, which is exemplified by the tumor suppressor proteins. It has been reported that many tumor suppressor proteins shuttle between the nucleus and the cytoplasm and that changes in this localization can have critical effects on their functions vis a vis the cell cycle, apoptosis and signaling path-ways.[52] Nucleocytoplasmic shuttling of tumor suppressor proteins, such as pRb and p27 can have important implications in cancer.[42] The PI3 Kinase-Akt pathway mediates the nuclear-cytoplasmic shuttling of many members of the FOXO family of transcription factors.[53] In addition, Akt has been shown to block the cell cycle inhibitory action of p27 through its phosphorylation at the nuclear localization sequence and subsequent retention in the cytosol.[46,54] Indeed, phosphorylation and cytosolic localization of p27 is associated with poor prognosis in many cancers.[55] Our data are consistent with the idea that, in the presence of PTP-regulated survival signaling, p27 is predominantly cytoplasmic. Nuclear import of p27 is also governed by its association with the 14~3~3 proteins and importin α.[56,57] Akt is known to affect the expression of 14-3-3 proteins by

exerting its inhibitory effects of the forkhead transcription factors, thereby providing another level of control to prevent nuclear re-entry of p27.[57]

Cancer cells often show deregulated signal transduction pathways that lead to inappropriate growth in response to external stimuli.[58] It has previously been reported that the PI3K/Akt pathway was involved in overriding G_2/M checkpoint arrest in the face of DNA damage.[59] However, there is little information regarding the role of Akt at the G_1/S transition. The G_1/S checkpoint exists to ensure that DNA damage is repaired before S-phase progression. Bypass of this checkpoint in the face of genotoxic stress can predispose cells to neoplastic progression, through the acquisition of mutations due to the replication of damaged DNA. Our findings indicate that Akt activation can bypass the G_1/S checkpoint induced by genotoxic exposure in normal human diploid cells. The significance of these findings is emphasized by the numerous reports linking Akt activation with tumor progression (review in refs. 59 and 60). Our work suggests that inappropriate Akt activation may also facilitate the early stages of oncogenesis after genotoxin exposure, via checkpoint bypass in normal cells. Moreover, Akt activation status may also be a key determinant of G_1/S checkpoint arrest in tumor cells in the face of chemotherapeutic genotoxin exposure. Therefore, a better knowledge of the regulation of the G_1/S checkpoint in normal cells is critical to understanding the molecular mechanisms underlying deregulation of cell cycle checkpoint control, and may lead to the development of targeted therapies.

Materials and Methods

Cell culture and reagents

Normal diploid human lung fibroblasts (HLFs, LL24, ATCC, Manassas, VA) were maintained in F12 complete medium, pH 7.2–7.4, containing antibiotics (penicillin 50 U/ml and streptomycin 50 μg/ml) and 15% fetal bovine serum (Hyclone Laboratories Inc., Logan, UT) in a 95% air and 5% CO_2 humidified atmosphere at 37°C. Unless otherwise specified, all chemicals were from Sigma (Sigma-Aldrich, St. Loius, MO) and of the highest purity available.

Treatment of cells with chromium

Sodium chromate ($Na_2CrO_4.4H_2O$, J.T. Baker Chemical Company, Philipsburg, NJ) stock solution was dissolved in double distilled water and sterilized by passage through a 0.2 μm filter before use. Cells were also treated with the protein tyrosine phosphatase (PTP) inhibitor, sodium orthovanadate (SOV; Na_3VO_4, Sigma-Aldrich, St. Louis, MO), which was also dissolved in double distilled water and sterilized through a 0.2 μm filter before use. In experiments in which SOV was co-incubated with Cr(VI), SOV was added 30 min prior to Cr(VI) addition.

Cell cycle analysis using bromodeoxyuridine (BrdU) and propidium iodide (PI) double staining

HLFs were seeded at a density of 5×10^5 cells/150 mm dish and incubated with 0, 1, 2 and 3 μM Cr(VI) with and without 10 μM SOV for 24 h. Cells were washed after treatment and maintained in F12 complete medium. At the indicated times, BrdU (Molecular Probes, Carlsbad, CA) was added to the medium at a final concentration of 10 μM, and cells were incubated for an additional 30 min. The cells were then trypsinized, washed with PBS and fixed in 70% ethanol. Following fixation, the cells were resuspended in 2 N HCl for 20 min and neutralized with 0.1 M sodium borate (pH 8.5) at room temperature. The cells were then incubated with an anti-BrdU monoclonal antibody (1:40 dilution, Molecular Probes, Invitrogen) for 30 min. The secondary antibody used was an Alexa Fluor 488 conjugated anti-mouse IgG (Molecular Probes). Cells were stained with 5 μg/ml PI in PBS and analyzed

using a flow cytometer (Becton Dickinson, Franklin Lakes, NJ). Alternatively, for a number of experiments, a BrdU FITC flow kit (BD Pharmingen) was used to determine BrdU incorporation, according to the manufacturers instructions. The wavelengths used were 488 nm for excitation, and the emission filters used were 530 nm for Alexa Fluor 488, 595 nm for PI and 650 nm for 7'AAD. The PI fluorescence signal (fluorescence pulse area versus pulse width) was used to exclude doublets and aggregates from analysis. The percentage of cells transitioning from G_1 to S phase was determined with 10,000 cells. The data were analyzed using the Cell Quest (Version 3.3) and the Modfit Mac LT (Version 3.1) software. In addition to the flow cytometry studies, cells were also analyzed for BrdU incorporation by immunofluorescence staining as described below.

Western blot

HLFs were seeded at a density of 1 × 10 cells/100 mm dish and were incubated at 37°C for 24 h prior to the indicated treatment. Following treatment, cells were lysed after 30 min incubation in TGN buffer (50 mM Tris (pH 7.5), 50 mM glycerophosphate, 150 mM NaCl, 10% glycerol, 1% Tween 20, containing 1 M NaF, 100 mM Na_3VO_4 and 2 μg/ml pepstatin A). In addition, 1 tablet of complete mini protease inhibitor (Roche, Basel, Switzerland) was added to every 10 ml of TGN buffer. The cells were lysed by sonication on ice for 5 second pulses at 40% amplitude. The lysates were then centrifuged at 12,000 rpm for 20 min at 2–8°C. Cytosolic and nuclear extracts from HLFs were prepared with a Nuclear Extraction Kit according to the manufacturer's instructions (Panomics, CA). The supernatants were resolved by 12% SDS-PAGE, transferred to polyvinylidene difluoride membranes (Perkin Elmer, Waltham, MA) and probed with the following antibodies: p21/WAF1 (Oncogene Research Products, San Diego, CA); p27/Kip1 (BD Transduction Laboratories, Franklin lakes, NJ); Cyclin D1 (Santa Cruz Biotechnology, Santa Cruz, CA); pRb Ser 807/811 (Cell Signaling Technology, Danvers, MA); Total Rb (Santa Cruz, biotechnology) and phospho Ser 473 Akt (Cell Signaling Technology) overnight. The membranes were then probed with the appropriate horseradish peroxidase-linked secondary antibody (Amersham Biosciences, Pittsburgh, PA). Secondary antibodies were visualized by ECL western blotting detection reagents (PerkinElmer). An antibody to either constitutively expressed β-actin or α-tubulin was used to confirm equal protein loading (Sigma).

Immunofluorescent detection of p21, p27, pRb, cyclin D1 and BrdU

HLFs were seeded at a density of 1 × 10 cells/well in 8 well chamber slides (Nunc International, Rochester, NY) and were incubated at 37°C for 24 h prior to the indicated treatment. The cells were rinsed with 200 μl of phosphate buffered saline (PBS) for 10 min, fixed with 100% methanol at ~20°C for 10 min, and then kept in the dark. The cells were sequentially rehydrated with 80%, 60%, 40% and 20% methanol in PBS, each for a duration of 10 min in the dark. The cells were washed with PBS and blocked with 3% BSA in PBS for 30 min or longer at room temperature. The cells were then rinsed with PBS and incubated with primary antibody diluted 1:250 in 3% BSA at 4°C overnight. Following incubation, the cells were rinsed with PBS and incubated for 1 h at room temperature with secondary antibody [goat anti-mouse IgG conjugated to Alexa Fluor 488 for mouse monoclonal primary antibodies (p21, p27, BrdU), and goat anti rabbit IgG conjugated to Alexa Fluor 488 for rabbit polyclonal primary antibodies (Cyclin D1, pRb)] at a 1:4,000 dilution in 3% BSA. The cells were then rinsed with PBS. DNA staining was performed by incubating the cells with 100 μl 5 μg/ml PI for 30 min in the dark. The cells were then rinsed with PBS and were visualized by either fluorescence or confocal microscopy. Immunofluorescence was quantified for each experiment by counting five fields per treatment group and quantifying the number of cells positive for nuclear p27, pRb and BrdU as a percentage of the total number of cells per field, respectively. The fluorescent microscope used was an Olympus 1×70 (Center Valley, PA) and the confocal microscope

was a BioRad Zeiss Confocal (Hercules, CA). The magnifications used were 40X and 60X respectively. The excitation wavelengths were 488 nm for Alexa-Fluor conjugated antibodies and for PI.

Determination of PTEN tyrosine phosphorylation

Immunoprecipitation for pan-phosphotyrosine was carried out using a Catch and Release Phosphotyrosine Immunoprecipitation Kit according to the manufacturer's instruction (Millipore, Billerica, MA). HLFs at 24 hr post-seeding were treated with 10 μM SOV or medium alone for 1 h and protein lysates were extracted as described previously. 700 μg of protein lysates were added to the spin column prepacked with IP capture resin. Then 4 μg of anti-phosphotyrosine 4G10 antibody or normal mouse IgG was added to the column and incubated on a rotator at room temperature for 30 minutes. After 3 washes, proteins were eluted from the column with a denatured elution buffer followed by immunoblotting with anti-PTEN antibody (Cell Signaling). Reverse immunoprecipitation was carried out by immunoblotting for pan-pTyrosine from the PTEN immunoprecipitation by utilizing a catch and release Reverse Immunoprecipitation System (Millipore).

Akt in-vitro kinase activity assay

HLFs were seeded at a density of 10^6 cells/100 mm dish before being treated 24 h later with 0–6 μM Cr(VI) for an additional 24 h. Cells were then lysed on ice in the presence of a cell lysis buffer (Cell Signaling Technology) followed by sonication (ten 5 second pulses at an amplitude of 40%). After microcentrifugation at 14,000 xg for 20 min, 200 μl of cell lysate was incubated with 20 μl immobilized Akt monoclonal antibody (clone# 1G1, Cell Signaling Technology) overnight at 4°C. The immunocomplexes were recovered by centrifugation at 14,000 xg for 30 sec and washed twice with 500 μl of kinase buffer (Cell Signaling Technology). Kinase reactions were initiated by resuspending washed beads in 50 μl of kinase buffer supplemented with 1 μl of 10 mM ATP (Cell Signaling Technology) and 1 μg of Gsk~3 fusion protein (Cell Signaling Technology) at 37°C. The reaction was stopped after 30 min by the addition of SDS sample buffer.

Transfection

Akt activation was blocked by two approaches; gene silencing using siRNA and Akt inactivation by transfection with an Akt kinase dead mutant. For all transfections, HLFs were serum starved 4 h prior to the experiment and transfections were performed using the Amaxa nucleofector system. For siRNA silencing, HLFs were transfected with either buffer, Akt1 SMARTPool siRNA, or Cy3 luciferase siRNA as a control (Dharmacon, Lafayette, CO), at 120 pmoles. The Akt1 kinase dead (KD) plasmid (pCMV6-Myc-Akt KD) was obtained from Dr. Philip Tsichlis at Tufts University School of Medicine. The plasmid control was pmax from Dharmacon. Akt1-KD plasmids were transfected at a final concentration of 1 μg. In a separate series of experiments cells were transfected with the constitutively active myristoylated Akt1 plasmid (pCMV6-Myr-HA-Akt1), obtained from Dr. Tsichlis, at a final concentration of 1 μg.

Transfection efficiency was determined for each experiment with 2 ug of a pmax-GFP plasmid (Amaxa) and evaluation of cells by fluorescence microscopy. The average transfection efficiency usually achieved was between 80–90%. For all experiments, protein was collected at the indicated times in order to confirm Akt knockdown/activation depending on the type of transfection performed.

Statistical analysis

Graph Pad Prism version 4.0 (San Diego, CA) was used to perform statistical analysis among different experimental groups. One way analysis of variance (ANOVA) with a Bonferroni post test was used when performing multiple sample comparisons, whereas a two tailed, unpaired t test was performed when comparing two experimental groups. The results are presented as mean ± standard error of the mean or standard deviation of the mean for all experiments, and for all statistical analysis, $p < 0.05$ was considered statistically significant unless stated otherwise.

Supplementary Material

Refer to Web version on PubMed Central for supplementary material.

Acknowledgments

The authors would like to thank Dr. Philip Tschlis at Tufts University for his generous gift of the constitutively active Myr-Akt plasmids as well as Dr. Travis O'Brien for his critical evaluation of this manuscript. We also thank Kristen Wright, Gina Chun and Dr. Laura Beaver for their valuable suggestions. This work was supported by NIH grants, CA107972 to S.C. and ES05304 and ES09961, to S.R.P.

Abbreviations

PTP	protein tyrosine phosphatase
SOV	sodium orthovanadate
HLF	human lung fibroblast
pRb	phospho Ser 807/811 Rb
Rb	retinoblastoma protein
Myr-Akt1	myristoylated Akt1
Akt1-KD	Akt1 kinase dead
PI	propidium iodide
7 AAD	7-amino actinomycin D
BrdU	bromodeoxyuridine

References

1. Satyanarayana A, Hilton MB, Kaldis P. p21 inhibits Cdk1 in the absence of Cdk2 to maintain the G_1/S phase DNA damage checkpoint. Mol Biol Cell. 2008; 19:65–77. [PubMed: 17942597]
2. Houtgraaf JH, Versmissen J, Van der Giessen WJ. A concise review of DNA damage checkpoints and repair in mammalian cells. Cardiovasc Revasc Med. 2006; 7:165–172. [PubMed: 16945824]
3. Hahn WC, Weinberg RA. Modelling the molecular circuitry of cancer. Nat Rev Cancer. 2002; 2:331–341. [PubMed: 12044009]
4. Vazquez F, Sellers WR. The PTEN tumor suppressor protein: an antagonist of phosphoinositide 3-kinase signaling. Biochim Biophys Acta. 2000; 1470:21–35.
5. Chu Y, Solski PA, Khosravi-Far R, Der CJ, Kelly K. The mitogen-activated protein kinase phosphatases PAC1, MKP-1 and MKP-2 have unique substrate specificities and reduced activity in vivo toward the ERK2 sevenmaker mutation. J Biol Chem. 1996; 271:6497–6501. [PubMed: 8626452]
6. Tonks NK. Protein tyrosine phosphatases: from genes, to function, to disease. Nat Rev Mol Cell Biol. 2006; 7:833–846. [PubMed: 17057753]

7. Ostman A, Hellberg C, Bohmer FD. Protein-tyrosine phosphatases and cancer. Nat Rev Cancer. 2006; 6:307–320. [PubMed: 16557282]
8. Wu DN, Pei DS, Wang Q, Zhang GY. Downregulation of PTEN by sodium orthovanadate inhibits ASK1 activation via PI3-K/Akt during cerebral ischemia in rat hippocampus. Neurosci Lett. 2006; 404:98–102. [PubMed: 16762504]
9. Schmid AC, Byrne RD, Vilar R, Woscholski R. Bisperoxovanadium compounds are potent PTEN inhibitors. FEBS Lett. 2004; 566:35–38. [PubMed: 15147864]
10. Chen WL, Harris DL, Joyce NC. Effects of SOV-induced phosphatase inhibition and expression of protein tyrosine phosphatases in rat corneal endothelial cells. Exp Eye Res. 2005; 81:570–580. [PubMed: 15950220]
11. Bae D, Camilli TC, Chun G, Lal M, Wright K, O'Brien TJ, et al. Bypass of hexavalent chromium-induced growth arrest by a protein tyrosine phosphatase inhibitor: Enhanced survival and mutagenesis. Mutat Res. 2009; 660:40–46. [PubMed: 19013184]
12. Al Aynati MM, Radulovich N, Ho J, Tsao MS. Overexpression of G_1-S cyclins and cyclin-dependent kinases during multistage human pancreatic duct cell carcinogenesis. Clin Cancer Res. 2004; 10:6598–6605. [PubMed: 15475449]
13. Havens CG, Ho A, Yoshioka N, Dowdy SF. Regulation of late G_1/S phase transition and APC Cdh1 by reactive oxygen species. Mol Cell Biol. 2006; 26:4701–4711. [PubMed: 16738333]
14. Mullany LK, White P, Hanse EA, Nelsen CJ, Goggin MM, Mullany JE, et al. Distinct proliferative and transcriptional effects of the D-type cyclins in vivo. Cell Cycle. 2008; 7:2215–2224. [PubMed: 18635970]
15. Sherr CJ, Roberts JM. CDK inhibitors: positive and negative regulators of G_1-phase progression. Genes Dev. 1999; 13:1501–1512. [PubMed: 10385618]
16. Arima Y, Hirota T, Bronner C, Mousli M, Fujiwara T, Niwa S, et al. Downregulation of nuclear protein ICBP90 by p53/$p21^{Cip1/WAF1}$-dependent DNA-damage checkpoint signals contributes to cell cycle arrest at G_1/S transition. Genes Cells. 2004; 9:131–142. [PubMed: 15009091]
17. Langard S. One hundred years of chromium and cancer: a review of epidemiological evidence and selected case reports. Am J Ind Med. 1990; 17:189–215. [PubMed: 2405656]
18. O'Brien TJ, Ceryak S, Patierno SR. Complexities of chromium carcinogenesis: role of cellular response, repair and recovery mechanisms. Mutat Res. 2003; 533:3–36. [PubMed: 14643411]
19. Langard S. One hundred years of chromium and cancer: a review of epidemiological evidence and selected case reports. Am J Ind Med. 1990; 17:189–215. [PubMed: 2405656]
20. O'Brien TJ, Ceryak S, Patierno SR. Complexities of chromium carcinogenesis: role of cellular response, repair and recovery mechanisms. Mutat Res. 2003; 533:3–36. [PubMed: 14643411]
21. Jiang X, Norman M, Li X. Use of an array technology for profiling and comparing transcription factors activated by TNFalpha and PMA in HeLa cells. Biochim Biophys Acta. 2003; 1642:1–8. [PubMed: 12972287]
22. Ha L, Ceryak S, Patierno SR. Generation of S phase-dependent DNA double-strand breaks by Cr(VI) exposure: involvement of ATM in Cr(VI) induction of gamma-H2AX. Carcinogenesis. 2004; 25:2265–2274. [PubMed: 15284180]
23. Ball KL, Lain S, Fahraeus R, Smythe C, Lane DP. Cell cycle arrest and inhibition of Cdk4 activity by small peptides based on the carboxy-terminal domain of $p21^{WAF1}$. Curr Biol. 1997; 7:71–80. [PubMed: 8999999]
24. Wallick CJ, Gamper I, Thorne M, Feith DJ, Takasaki KY, Wilson SM, et al. Key role for $p27^{Kip1}$, retinoblastoma protein Rb, and MYCN in polyamine inhibitor-induced G_1 cell cycle arrest in MYCN-amplified human neuroblastoma cells. Oncogene. 2005; 24:5606–5618. [PubMed: 16007177]
25. Scheving LA, Thomas JR, Zhang L. Regulation of intestinal tyrosine phosphorylation and programmed cell death by peroxovanadate. Am J Physiol. 1999; 277:572–579.
26. Rosivatz E, Matthews JG, McDonald NQ, Mulet X, Ho KK, Lossi N, et al. A small molecule inhibitor for phosphatase and tensin homologue deleted on chromosome 10 (PTEN). ACS Chem Biol. 2006; 1:780–790. [PubMed: 17240976]
27. De Vita G, Berlingieri MT, Visconti R, Castellone MD, Viglietto G, Baldassarre G, et al. Akt/protein kinase B promotes survival and hormone-independent proliferation of thyroid cells in the

absence of dedifferentiating and transforming effects. Cancer Res. 2000; 60:3916–3920. [PubMed: 10919669]

28. Blume-Jensen P, Hunter T. Oncogenic kinase signalling. Nature. 2001; 411:355–365. [PubMed: 11357143]
29. Hahn WC, Weinberg RA. Modelling the molecular circuitry of cancer. Nat Rev Cancer. 2002; 2:331–341. [PubMed: 12044009]
30. Landgren E, Blume-Jensen P, Courtneidge SA, Claesson-Welsh L. Fibroblast growth factor receptor-1 regulation of Src family kinases. Oncogene. 1995; 10:2027–2035. [PubMed: 7761103]
31. Smith JB. Vanadium ions stimulate DNA synthesis in Swiss mouse 3T3 and 3T6 cells. Proc Natl Acad Sci USA. 1983; 80:6162–6166. [PubMed: 6353410]
32. Jones TR, Reid TW. Sodium orthovanadate stimulation of DNA synthesis in Nakano mouse lens epithelial cells in serum-free medium. J Cell Physiol. 1984; 121:199–205. [PubMed: 6384242]
33. Scheving LA, Thomas JR, Zhang L. Regulation of intestinal tyrosine phosphorylation and programmed cell death by peroxovanadate. Am J Physiol. 1999; 277:572–579.
34. Matsumoto J, Morioka M, Hasegawa Y, Kawano T, Yoshinaga Y, Maeda T, et al. Sodium orthovanadate enhances proliferation of progenitor cells in the adult rat subventricular zone after focal cerebral ischemia. J Pharmacol Exp Ther. 2006; 318:982–991. [PubMed: 16782823]
35. Feng Y, Bhatt AJ, Fratkin JD, Rhodes PG. Neuroprotective effects of sodium orthovanadate after hypoxic-ischemic brain injury in neonatal rats. Brain Res Bull. 2008; 76:102–108. [PubMed: 18395618]
36. Wu DN, Pei DS, Wang Q, Zhang GY. Downregulation of PTEN by sodium orthovana-date inhibits ASK1 activation via PI3-K/Akt during cerebral ischemia in rat hippocampus. Neurosci Lett. 2006; 404:98–102. [PubMed: 16762504]
37. Matsumoto J, Morioka M, Hasegawa Y, Kawano T, Yoshinaga Y, Maeda T, et al. Sodium orthovanadate enhances proliferation of progenitor cells in the adult rat subventricular zone after focal cerebral ischemia. J Pharmacol Exp Ther. 2006; 318:982–991. [PubMed: 16782823]
38. Feng Y, Bhatt AJ, Fratkin JD, Rhodes PG. Neuroprotective effects of sodium orthovana-date after hypoxic-ischemic brain injury in neonatal rats. Brain Res Bull. 2008; 76:102–108. [PubMed: 18395618]
39. Yang P, Dankowski A, Hagg T. Protein tyrosine phosphatase inhibition reduces degeneration of dopaminergic substantia nigra neurons and projections in 6-OHDA treated adult rats. Eur J Neurosci. 2007; 25:1332–1340. [PubMed: 17425559]
40. Bhuiyan MS, Takada Y, Shioda N, Moriguchi S, Kasahara J, Fukunaga K. Cardioprotective effect of vanadyl sulfate on ischemia/reperfusion-induced injury in rat heart in vivo is mediated by activation of protein kinase B and induction of FLICE-inhibitory protein. Cardiovasc Ther. 2008; 26:10–23. [PubMed: 18466417]
41. Muranaka S, Kanno T, Fujita H, Kobuchi H, Akiyama J, Yasuda T. Involvement of ceramide in the mechanism of Cr(VI)-induced apoptosis of CHO cells. Free Radic Res. 2004; 38:613–621. [PubMed: 15346652]
42. Jiao W, Datta J, Lin HM, Dundr M, Rane SG. Nucleocytoplasmic shuttling of the retinoblastoma tumor suppressor protein via Cdk phosphorylation-dependent nuclear export. J Biol Chem. 2006; 281:38098–38108. [PubMed: 17043357]
43. Guo J, Sheng G, Warner BW. Epidermal growth factor-induced rapid retinoblastoma phosphorylation at Ser780 and Ser795 is mediated by ERK1/2 in small intestine epithelial cells. J Biol Chem. 2005; 280:35992–35998. [PubMed: 16126730]
44. Weitzman JB, Fiette L, Matsuo K, Yaniv M. JunD protects cells from p53-dependent senescence and apoptosis. Mol Cell. 2000; 6:1109–1119. [PubMed: 11106750]
45. Zhang QG, Wu DN, Han D, Zhang GY. Critical role of PTEN in the coupling between PI3K/Akt and JNK1/2 signaling in ischemic brain injury. FEBS Lett. 2007; 581:495–505. [PubMed: 17239858]
46. Kao ST, Yeh CC, Hsieh CC, Yang MD, Lee MR, Liu HS, et al. The Chinese medicine Bu-Zhong-Yi-Qi-Tang inhibited proliferation of hepatoma cell lines by inducing apoptosis via G_0/G_1 arrest. Life Sci. 2001; 69:1485–1496. [PubMed: 11554610]

47. Berns K, Martins C, Dannenberg J, Berns A, Bernards R. $p27^{kip1}$-independent cell cycle regulation by MYC. Oncogene. 2000; 19:4822–4827. [PubMed: 11039898]
48. Sugimoto M, Martin N, Wilks DP, Tamai K, Huot TJ, Pantoja C, et al. Activation of cyclin D1-kinase in murine fibroblasts lacking both p21(Cip1) and p27(Kip1). Oncogene. 2002; 21:8067–8074. [PubMed: 12444543]
49. Ceryak S, Zingariello C, O'Brien T, Patierno SR. Induction of pro-apoptotic and cell cycle-inhibiting genes in chromium (VI)-treated human lung fibroblasts: lack of effect of ERK. Mol Cell Biochem. 2004; 255:139–149. [PubMed: 14971655]
50. Coqueret O. New roles for p21 and p27 cell cycle inhibitors: a function for each cell compartment? Trends Cell Biol. 2003; 13:65–70. [PubMed: 12559756]
51. Miao LJ, Wang J, Li SS, Wu YM, Wu YJ, Wang XC. Correlation of p27 expression and localization to phosphorylated AKT in non-small cell lung cancer. Ai Zheng. 2006; 25:1216–1220. [PubMed: 17059763]
52. Salmena L, Pandolfi PP. Changing venues for tumour suppression: balancing destruction and localization by monoubiquitylation. Nat Rev Cancer. 2007; 7:409–413. [PubMed: 17508027]
53. Jang SW, Yang SJ, Srinivasan S, Ye K. Akt phosphorylates MstI and prevents its proteolytic activation, blocking FOXO3 phosphorylation and nuclear translocation. J Biol Chem. 2008; 282:30836–30844. [PubMed: 17726016]
54. Shin I, Rotty J, Wu FY, Arteaga CL. Phosphorylation of $p27^{Kip1}$ at Thr-157 interferes with its association with importin alpha during G_1 and prevents nuclear re-entry. J Biol Chem. 2005; 280:6055–6063. [PubMed: 15579463]
55. Newman L, Xia W, Yang HY, Sahin A, Bondy M, Lukmanji F, et al. Correlation of p27 protein expression with HER-2/neu expression in breast cancer. Mol Carcinog. 2001; 30:169–175. [PubMed: 11301477]
56. Shin I, Yakes FM, Rojo F, Shin NY, Bakin AV, Baselga J, et al. PKB/Akt mediates cell cycle progression by phosphorylation of p27(Kip1) at threonine 157 and modulation of its cellular localization. Nat Med. 2002; 8:1145–1152. [PubMed: 12244301]
57. Sekimoto T, Fukumoto M, Yoneda Y. 14-3-3 suppresses the nuclear localization of threonine 157-phosphorylated p27(Kip1). EMBO J. 2004; 23:1934–1942. [PubMed: 15057270]
58. Nakanishi M, Shimada M, Niida H. Genetic instability in cancer cells by impaired cell cycle checkpoints. Cancer Sci. 2006; 97:984–989. [PubMed: 16925578]
59. Kandel ES, Hay N. The regulation and activities of the multifunctional serine/threonine kinase Akt/PKB. Exp Cell Res. 1999; 253:210–229. [PubMed: 10579924]
60. Crowell JA, Steele VE, Fay JR. Targeting the AKT protein kinase for cancer chemoprevention. Mol Cancer Ther. 2007; 6:2139–2148. [PubMed: 17699713]

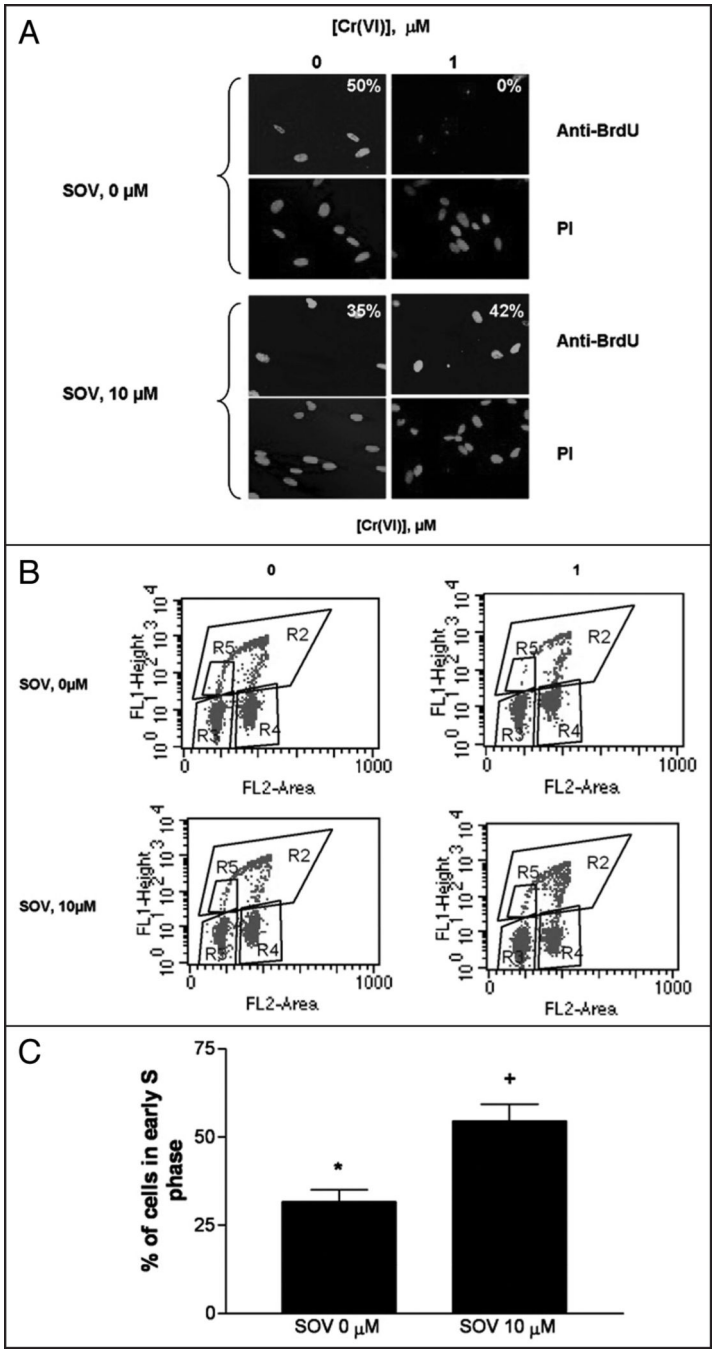

Figure 1.

G_1/S checkpoint arrest is bypassed by PTP inhibition. HLF cells were incubated with 0 or 1 μM Cr(VI) in the presence and absence of 10 μM SOV for 24 h and cells were treated with BrdU for 30 minutes before collection and fixation. Cells were fixed and incubated with mouse anti-BrdU antibody and Alexa 488-conjugated goat anti mouse secondary antibody and DNA was stained with PI. (A) HLF cells were seeded on chamber slides prior to treatement. All pictures were taken on an Olympus 1×70 fluorescence microscope at a magnification level of 40X. The numbers indicate the percentage of cells positive for BrdU incorporation, and are the means of 2 experiments. (B) Dot plots show the incorporation of BrdU into DNA (y axis) as an indication of DNA synthesis and PI fluorescence (x axis) as

an indication of DNA content. (C) The percentage of total cells in early S phase as assessed by BrdU incorporation was quantified from region R5 in Figure 1B. Data are mean ± SE of four experiments and are expressed as percentage of total cells, normalized to respective control. *indicates a statistically significant difference from control ($p < 0.05$) and $^{+}$indicates a statistically significant difference between the samples treated with and without SOV ($p < 0.05$).

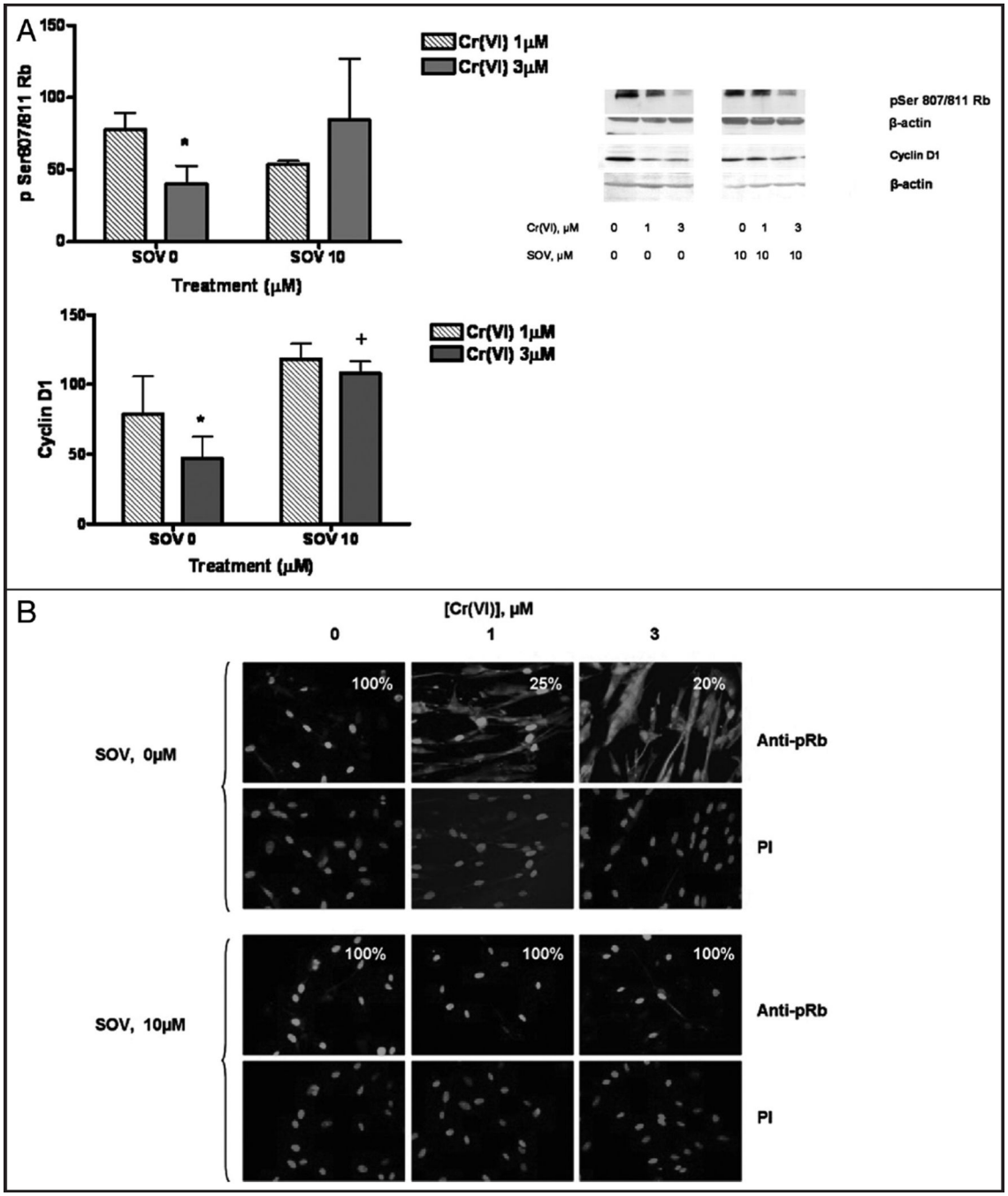

Figure 2.

The PTP inhibitor-induced bypass of the G_1/S checkpoint is associated with changes in pRb and Cyclin D1 protein expression and pRB cellular localization. HLF cells were treated with 0, 1 or 3 μM Cr in the presence and absence of 10 μM SOV for 24 h. Total cellular protein was extracted after the treatment. (A) Proteins were separated by SDS-PAGE and total pSer 807/811 Rb and Cyclin D1 were detected by immunoblotting. The same amount of protein loading was confirmed by immunoblotting for β-actin. Data are the means ± SE of three independent experiments and are expressed as percentage of control, normalized to β-actin. *indicates a statistically significant difference from control ($p < 0.05$) and $^{+}$indicates a statistically significant difference between the samples treated with and without SOV ($p <$

0.05). (B) HLF cells were seeded on chamber slides and, after treatment, were fixed and incubated with rabbit pRb antibody and Alexa 488-conjugated goat anti-rabbit secondary antibody. DNA was stained with PI to indicate the position of the nucleus. The numbers in each box represent the percent of cells that have exclusive nuclear pRb.

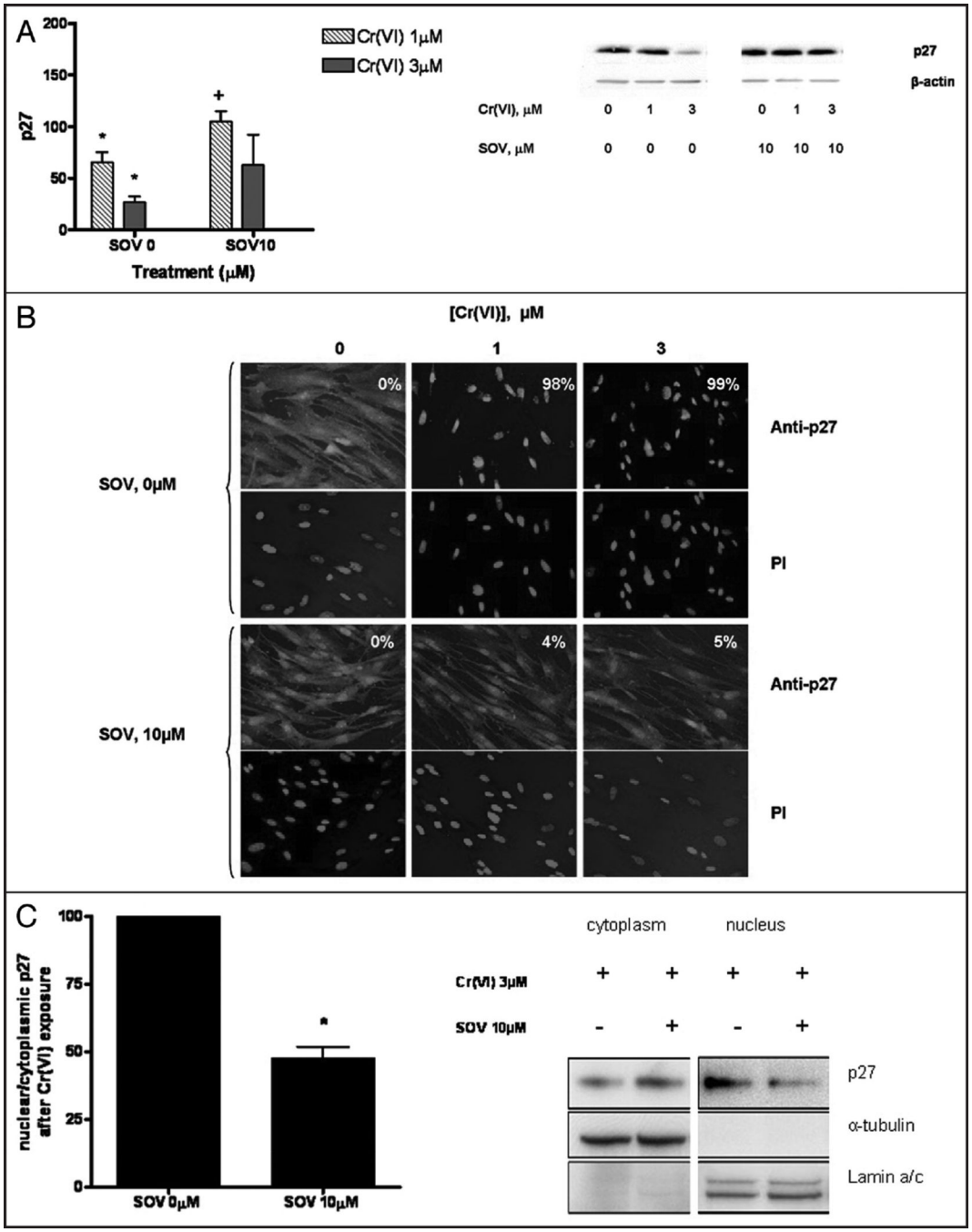

Figure 3.

The PTP inhibitor-induced bypass of the G_1/S checkpoint is associated with changes in p27 protein expression and cellular localization. HLF cells were treated with 0, 1 or 3 μM Cr in the presence and absence of 10 μM SOV for 24 h. Total cellular protein was extracted after the treatment. (A) Proteins were separated by SDS-PAGE and total p27 was detected by immunoblotting. The same amount of protein loading was confirmed by immunoblotting for β-actin. Data are the means ± SE of three independent experiments and are expressed as percentage of control, normalized to β-actin. *indicates a statistically significant difference from control ($p < 0.05$) and $^{+}$indicates a statistically significant difference between the samples treated with and without SOV ($p < 0.05$). (B) HLF cells were seeded on chamber

slides and, after treatment, were fixed and incubated with mouse p27 antibody and Alexa 488-conjugated goat anti-mouse secondary antibody. DNA was stained with PI to indicate the position of the nucleus. The numbers in each box represent the % of cells that have p27 nucleo-cytoplasmic localization. (C) Immunoblotting of the nuclear and cytoplasmic fractions for p27. α-Tubulin and Lamin A/C are loading controls for the cytoplasmic and nuclear fractions respectively. Data are mean ± SE of four experiments and are expressed as percentage of SOV 10 μM control. *indicates a statistically significant difference from control ($p < 0.05$).

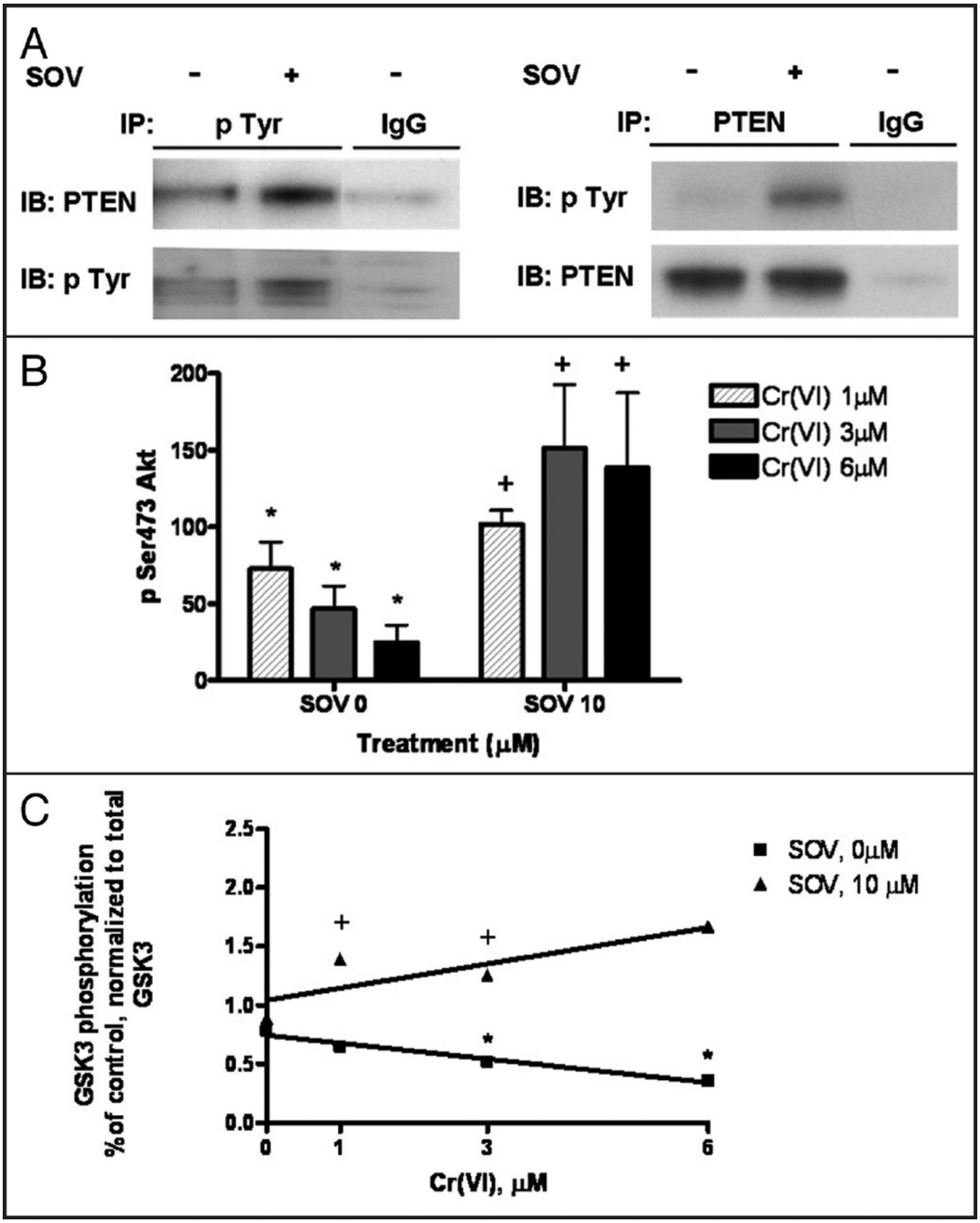

Figure 4.

PTP inhibition abrogates the Cr(VI)-induced decrease in Akt expression and activity. (A) HLF cells were treated with and without 10 μM SOV for 1 h. Total protein was extracted and immunoblotting for PTEN from the pan-pTyrosine immunoprecipitates and for pTyrosine from the PTEN immnuoprecipitates was performed. Non specific IgG was used as the negative control. (B) HLF cells were treated with 0, 1, 3 or 6 μM Cr in the presence and absence of 10 μM SOV for 24 h. Total cellular protein was extracted after the treatment. Proteins were separated by SDS-PAGE and total pSer 473 Akt was detected by immunoblotting. The same amount of protein loading was confirmed by immunoblotting for β-actin. Data are the means ± SE of three independent experiments and are expressed as

percentage of control, normalized to β-actin. * indicates a statistically significant difference from control ($p < 0.05$) and $^{+}$ indicates a statistically significant difference between the samples treated with and without SOV ($p < 0.05$). (C) HLF cells were treated with 0, 1, 3 or 6 μM Cr in the presence and absence of 10 μM SOV for 24 h. Total cellular protein was extracted, and Akt was immunoprecipitated and used in an in vitro kinase assay with a Gsk-3 fusion protein as a substrate. Proteins from each reaction were separated by SDS-PAGE, and Gsk-3 phosphorylation was detected by immunoblotting, and normalized to total Gsk-3 protein expression. Data are the means ± SE of two independent experiments are expressed as percentage of control, normalized to total GSK3 and + indicates a statistically significant difference between samples treated with and without SOV ($p < 0.05$). Cr(VI) induced a statistically significant ($p < 0.05$) decrease in Akt in vitro activity as determined by linear regression analysis ($r^2 = 0.9647$).

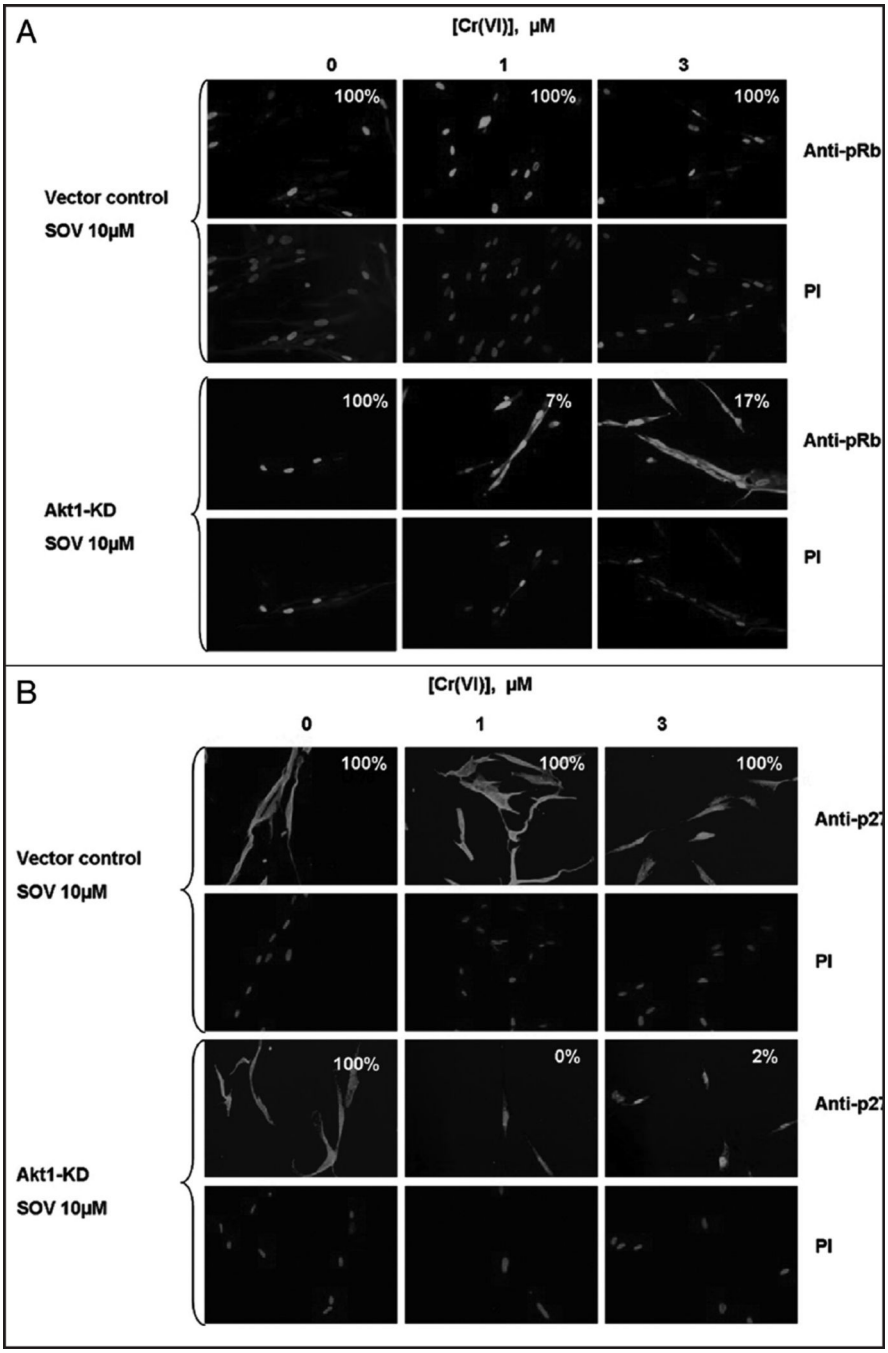

Figure 5.

Akt is necessary for the PTP inhibitor-induced abrogation of Cr(VI)-induced effects on the localization of pRb and p27. (A) HLF cells transfected with vector control and Akt1-KD plasmids were incubated with 0, 1 and 3 μM Cr(VI) in the presence and absence of 10 μM SOV for 24 h. Cells were fixed and incubated with rabbit pRb antibody and Alexa 488-conjugated goat anti rabbit secondary antibody. DNA was stained using PI to indicate the position of the nucleus. The numbers in each box represent the % of cells that have exclusive nuclear pRb. (B) HLF cells transfected with vector control and Akt1 Kinase dead plasmids and were incubated with 0, 1 and 3 μM Cr(VI) in the presence and absence of 10 μM SOV for 24 h. Cells were fixed and incubated with a mouse p27 antibody and Alexa

488-conjugated goat anti mouse secondary antibody. DNA was stained with PI to indicate the position of the nucleus. The numbers in each box represent the % of cells that have p27 nucleo-cytoplasmic localization. All pictures were taken on an Olympus 1×70 fluorescence microscope at a magnification level of 40X.

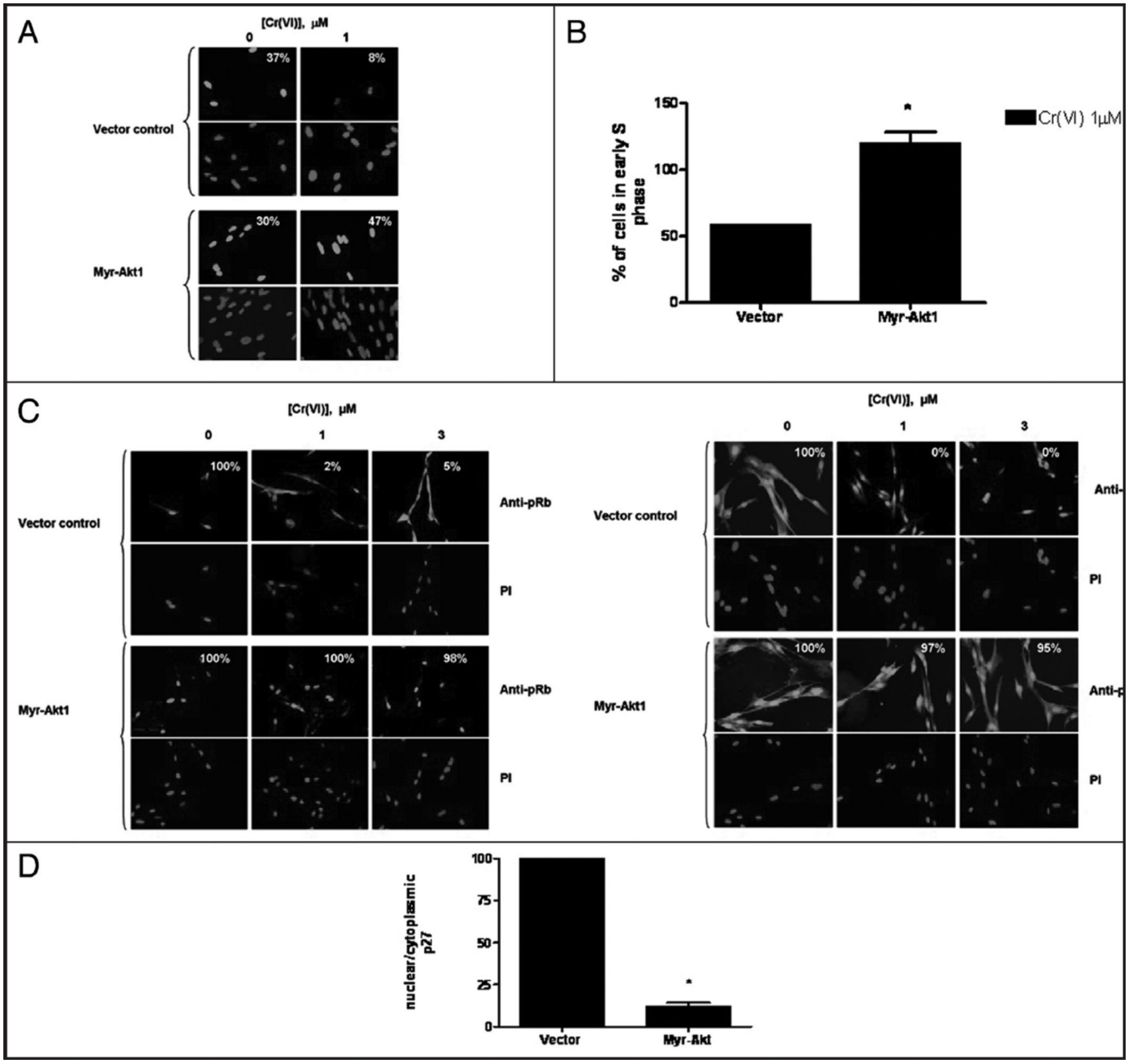

Figure 6.

Akt is sufficient for G_1/S checkpoint bypass and G_1/S effector re-localization after Cr(VI) exposure. HLF cells transfected with either the vector control or the constitutively active Myr-Akt1 plasmid were incubated with 0 or 1 μM Cr(VI) for 24 h. (A) Transfected HLF cells were seeded on chamber slides and were incubated with 0 or 1 μM Cr(VI) for 24 h and incubated with BrdU for the final 30 minutes. Cells were fixed and incubated with mouse anti-BrdU antibody and FITC-conjugated goat anti-mouse secondary antibody. Cells were treated with PI to stain the DNA. All pictures were taken on an Olympus 1×70 fluorescence microscope at a magnification level of 40X. The numbers indicate the percentage of cells positive for BrdU incorporation, and are representative of one experiment. (B) Cells were fixed and labeled with mouse anti-BrdU antibody and AAD to stain the DNA. The graphical representation of the flow cytometry data shows the number of cells in early S-phase in the

vector and Myr-Akt1 transfected cells treated with 1 μM Cr(VI). Data are the means ± SE of two experiments and *indicates a statistically significant difference from the vector control treated with 1 μM. (C) HLF cells transfected with the vector and constitutively active Myr-Akt1 plasmid were seeded on chamber slides and were incubated with 0, 1 or 3 μM Cr(VI) for 24 h. Cells were fixed and incubated with either the rabbit pRb antibody or the mouse anti p27 antibody and Alexa 488-conjugated goat anti rabbit or anti mouse secondary antibody, respectively. DNA was stained with PI to indicate the position of the nucleus. All pictures were taken on an Olympus 1×70 fluorescence microscope at a magnification level of 40X. The numbers in each box represent the % of cells that have exclusive nuclear pRb, and the % of cells that have p27 nucleo-cytoplasmic localization, respectively. (D) Immunoblotting of p27 in nuclear and cytoplasmic fractions in vector and Myr-Akt1 transfected cells. α-Tubulin and Lamin a/c are loading controls for the cytoplasmic and nuclear fractions, respectively. Data are mean ± SE of four experiments and are expressed as percentage of Myr-Akt1 transfected control. *indicates a statistically significant difference from control ($p < 0.05$).